Scaling PRI between coniferous canopy structures

Matti Mõttus and Miina Rautiainen

***Abstract*—We measured simultaneously the spectral albedo of ten Scots pine shoots and the needles constituting the shoots. Next, we used the spectral information to calculate the photochemical reflectance index (PRI) which allows to retrieve photosynthetic productivity from imaging spectroscopy data. We showed that PRI can be scaled from needle to shoot level using a strictly positive scaling factor. The scaling factor is a function of photon recollision probability and the harmonic mean of needle spectral albedos at the wavelengths used in the index. The method is applicable to other normalized difference indices, as demonstrated here using NDVI. At shoot level, both PRI and NDVI depend on the angle between view and illumination directions. This anisotropy, however, is not a direct function of scattering angle.**

***Index Terms*—*Pinus sylvestris*, Scots pine, Photochemical Reflectance Index, vegetation structure, shoot scattering, photon recollision probability**

I. Introduction

Leaf-level photosynthetic efficiency can be estimated by measuring leaf reflectance at 531 nm [1]. This spectral region reveals physiological adaptations aimed at coping with excess photosynthetically active radiation: interconversion of the xanthophyll cycle pigments, and reversible chloroplast conformation changes. Thus, the photochemical reflectance index

$$\mathrm{PRI} = \frac{\omega(531) - \omega(570)}{\omega(531) + \omega(570)} \quad (1)$$

was proposed, where ω is leaf spectral albedo and the number in parentheses denotes wavelength in nanometers. In (1), 570 nm is a reference wavelength used to reduce the effect of natural variation in leaf optical properties on the value of the index. The usefulness of PRI has been demonstrated for interpreting canopy level spectroradiometric measurements [2] as well as remote sensing data [3]. PRI is considered one of the most promising candidates for retrieving information on photosynthetic activity from space [4]. Monitoring photosynthesis from satellites requires scaling the PRI measured for the whole vegetation canopy to the level of a single leaf (or, in the case of conifers, a needle), where the connection between light absorption at 531 nm and xantophyll cycle pigments has been established. Unfortunately, the value of PRI recorded by a remote sensing instrument depends on view and illumination geometry, and the correlation between PRI and productivity (i.e., carbon uptake) on vegetation structure [2], [3], [5]. The effect of vegetation structure on its reflectance complicates the retrieval of foliar biochemistry from remote sensing data (e.g., [6], [7], [8]) and is one of the key factors hindering the operational use of PRI in estimating vegetation productivity from space [4]. An example of vegetation structure is the grouping of needles into shoots. Indeed, it is impossible to distinguish the contributions of separate needles in the optical signal of any air- or space-bourne remote sensing instrument. In conifers, the shoot is usually considered the basic scattering element (e.g., [9], [10], [11]) and thus, the effect of shoot-level grouping has to be accounted for when interpreting the PRI signal.

Recently, it has been demonstrated that multiangular measurements can be used to overcome many complications associated with utilization of canopy-level PRI. Instead of the value of PRI, the difference in the index measured at different view angles can be used to estimate canopy productivity [2], [12], [13]. The approach is based on measuring the difference between PRI for sunlit and shaded leaves by relating view angle to the fraction of visible sunlit foliage. Unless proven otherwise, the PRI of a sunlit (or, equivalently, shaded) conifer shoot cannot be assumed to be independent of the angle from which it is viewed. For example, the scattering properties of Scots pine shoots are strongly anisotropic, and while the scattering directionality is relatively independent of wavelength [14], this cannot be expected to hold for all directions or specific wavelengths. However, we have not found any earlier reports on the direct effect of viewing direction on the recorded value of the index.

Mathematically, PRI belongs to the family of normalized difference indices (NDIs) calculated by dividing the difference of the optical signal at two wavelengths by the corresponding sum. The best-known of these is the normalized difference vegetation index (NDVI) [15]. Other NDIs have been developed to investigate different properties of green vegetation [16]. For example, the NDWI [17] measures vegetation water content, SIWSI soil moisture and vegetation moisture stress [18], and VI_{green} was designed to determine vegetation fraction [19]. The wavelengths used in these indices vary. However, due to their similarity, the mathematical effect of vegetation structure on these indices will be identical.

In this paper, we present a simple method for scaling narrowband NDIs such as PRI in coniferous canopies from needle to shoot level, and vice versa. In addition, we describe the anisotropy (i.e. directional variation) in shoot-level PRI. To illustrate the general nature of the scaling method, we also briefly compare the scaling properties and shoot-level anisotropy of PRI to those of NDVI, the most commonly used vegetation index.

M. Mõttus is with University of Helsinki, Department of Geosciences and Geography, P.O. Box 64, FI-00014 University of Helsinki, Finland (corresponding author, email: matti.mottus@helsinki.fi)

M. Rautiainen is with University of Helsinki, Department of Forest Sciences, P.O. Box 27, FI-00014 University of Helsinki, Finland

This research was funded by Postdoctoral Funds of University of Helsinki and the Academy of Finland.

II. Materials and Methods

A. Laboratory measurements

All measurements were carried out in the facilities of Remote Sensing Laboratories (RSL), University of Zurich, Switzerland in March 2011 . Ten shoots were sampled from Scots pine (*Pinus sylvestris* L.) trees growing near the campus area so that they covered a wide range of canopy locations. Each sample consisted of two sister-shoots, i.e., same-year shoots growing next to each other. From the sister-shoots, one shoot was used for measuring shoot structural and spectral properties, and the other shoot for measuring simultaneously needle optical properties. Shoots were picked in the morning and stored in a cool dark place until the optical measurements in the same day. For each shoot we measured also the basic structural properties and calculated the ratio of the average shoot silhouette area to total needle area ($\overline{\text{STAR}}$).

The aim of optical measurements was to determine the spectral single-scattering albedo of needles and shoots, $\omega_n(\lambda)$ and $\omega_{sh}(\lambda)$, respectively. The spectral single-scattering albedo $\omega(\lambda)$ of a vegetation canopy element is defined as the fraction of intercepted monochromatic radiation with wavelength λ not absorbed by the canopy element. For brevity, the term single-scattering is dropped from here onwards and we will refer to $\omega(\lambda)$ as spectral albedo.

Directional shoot scattering was measured with an ASD Fieldspec 3 spectroradiometer mounted on the LAGOS goniometer system [20] in an optically black laboratory. We used an angular sampling pattern based on Gauss–Legendre quadrature over the cosine of the polar angle and uniform sampling of the azimuth angle. The total number of quadrature nodes on the full sphere was 72. The illumination source was a 1000 W brightness-stabilized quartz tungsten halogen lamp providing irradiance levels close to that in a beam of direct sunlight. The usable spectral range, limited by lamp spectrum and the sensitivity of the spectroradiometer, was 400 to 2000 nm. The equipment did not allow us to measure shoot scattering in the exact backscatter and forwardscatter directions. Full details of the measurement setup are given in [14]. Before and after measuring each shoot, we recorded the reflectance signal produced by a small Spectralon panel placed in the center of the goniometer. Spectralon measurements allowed us to calculate the theoretical signal produced by an isotropically scattering object with the same cross-section as the shoot. By dividing the measured signal with the theoretical one, we obtained the directional-spectral shoot scattering coefficient $\omega_{sh}(\lambda, \Omega)$. Finally, $\omega_{sh}(\lambda, \Omega)$ was integrated over the whole sphere to obtain the shoot spectral albedo $\omega_{sh}(\lambda)$.

The spectral albedos of needles in the sister-shoot were measured concurrently in a calibration laboratory using a second ASD FieldSpec 3 spectroradiometer and an RTS-3ZC integrating sphere. Three needle samples were prepared per shoot. Each sample consisted of eight to ten randomly selected needles, which were placed parallel to each other at a distance of less than the width of a needle in a specially designed needle sample carrier. Needle reflectance and transmittance measurements were used to calculate the needle spectral albedo $\omega_n(\lambda)$. During the measurements, both shoots and needles were exposed to irradiance levels close to that of natural sunlight. The measurements are described in full detail in [21].

The directional-spectral shoot scattering coefficients $\omega_{sh}(\lambda, \Omega)$ were used to calculate the directional shoot-level normalized difference indices $\text{PRI}_{sh}(\Omega)$ and $\text{NDVI}_{sh}(\Omega)$. Using the shoot spectral albedo $\omega_{sh}(\lambda)$ in (1) or (2) resulted in the spherically averaged shoot-level indices, PRI_{sh} and NDVI_{sh}, respectively. As the directionality of needle scattering was not measured, we calculated only the spherically averaged needle-level indices PRI_n and NDVI_n using the needle spectral albedo $\omega_n(\lambda)$. The wavelengths used in PRI are given in (1). We used a narrow-band version of NDVI calculated as

$$\text{NDVI} = \frac{\omega(780) - \omega(680)}{\omega(780) + \omega(680)}. \tag{2}$$

B. Scaling algorithm

To characterize the effect of shoot structure on the two vegetation indices we used the photon recollision probability theory. This theory states that the spectral albedo of a shoot ($\omega_{sh}(\lambda)$) is related to that of a needle ($\omega_n(\lambda)$) for all wavelengths λ as

$$\omega_{sh}(\lambda) = \frac{(1-p)\,\omega_n(\lambda)}{1 - p\omega_n(\lambda)}, \tag{3}$$

where p is photon recollision probability defined as the probability that a photon, which has been scattered by a needle in a shoot, will interact with the same shoot at least one more time [22]. The wavelength-independent probability p was calculated as

$$p = 1 - 4\overline{\text{STAR}}, \tag{4}$$

where $\overline{\text{STAR}}$ is the ratio of the measured average shoot silhouette area to total shoot needle area [22]. The p-theory has been verified both using computer simulations [22] and empirical measurements [21].

For a normalized shoot-level difference index NDI_{sh} (such as (1) or (2)), we obtain from (3)

$$\begin{aligned} \text{NDI}_{sh} &= \frac{\omega_{sh}(\lambda_2) - \omega_{sh}(\lambda_1)}{\omega_{sh}(\lambda_2) + \omega_{sh}(\lambda_1)} \\ &= \text{NDI}_n \times \frac{1}{1 - p\,W_n}, \end{aligned} \tag{5}$$

where

$$W_n = \frac{2}{\frac{1}{\omega_n(\lambda_1)} + \frac{1}{\omega_n(\lambda_2)}} \tag{6}$$

is the harmonic mean of the needle albedos ($\omega_n(\lambda_1)$ and $\omega_n(\lambda_2)$) at the two wavelengths (λ_1, λ_2) used in the index.

We used two methods to model the average shoot-level index value. First, we used all data available to us, i.e., we used the measured needle spectral albedo and the measured shoot-specific $\overline{\text{STAR}}$. Second, we averaged the needle spectral albedos over all shoots and used the average needle spectral albedo $\overline{\omega_n}(\lambda)$ in (5) while retaining the individual $\overline{\text{STAR}}$ value for each shoot. This was done to estimate the effect of shoot structure on the index.

C. Directional dependence of vegetation indices

Next, we analyzed the directionality of the two NDIs. For each shoot, we calculated Pearson's correlation coefficient R between the directional NDIs ($\mathrm{PRI}_{sh}(\Omega)$ and $\mathrm{NDVI}_{sh}(\Omega)$, Ω is the scattering direction) and shoot directional-spectral scattering coefficient $\omega_{sh}(\lambda, \Omega)$ for each wavelength. Due to the small number of shoots and considerable noise levels [14] leading to potential outliers, we chose the median correlation coefficient for each wavelength, together with the minimum and maximum values to characterize the spectral dependence of correlation. Thus, we obtained median correlation coefficients $\widetilde{R}_{PRI}(\lambda)$ and $\widetilde{R}_{NDVI}(\lambda)$ as functions of wavelength. To compare $\widetilde{R}_{NDI}(\lambda)$ with shoot spectra, we also calculated the median shoot albedo for each wavelength. For each wavelength, we tested for the statistical significance of the regression ($\mathrm{NDI}_{sh}(\Omega)$ vs. $\omega_{sh}(\lambda, \Omega)$) at the significance level $\alpha = 0.05$.

Similarly, we tested for a correlation of $\mathrm{NDI}_{sh}(\Omega)$ with the scattering direction Ω. Shoot scattering can be efficiently described using a bi-Lambertian model which describes total shoot scattering as the sum of two components: isotropic and Lambertian [14]. While isotropic scattering contributes equally to all directions, the Lambertian component enhances shoot scattering in backward directions only. As the name implies, the Lambertian component introduces a linear dependence between the cosine of the scattering angle ϑ (the angle between Ω and incidence direction, $\vartheta = 180^\circ$ equals exact backscatter direction). Thus, we looked for a correlation and a statistically significant regression between the directional $\mathrm{NDI}(\Omega)$ and $\cos\vartheta$ separately for $\vartheta < 90^\circ$ (forward-scattering directions) and $\vartheta > 90^\circ$ (backward-scattering directions).

III. Results and discussion

A. Scaling PRI and NDVI

According to (5), scaling from needle to shoot level is accomplished by multiplying NDI_n by the scaling factor $\frac{1}{1-p\,W_n}$. This factor is a function of the shoot structural parameter p and the mean needle albedo W_n. For small values of p and W_n, the scaling factor is close to unity. This corresponds to sparse shoots (low probability of hitting needles within the same shoot again) and wavelengths where needle pigments or its other constituents absorb. For the two indices studied here, the harmonic means (6) are almost equal ($W_{n,\mathrm{PRI}} = 0.27$, $W_{n,\mathrm{NDVI}} = 0.26$) and p varied between 0.24 and 0.52 [21]. Thus, the scaling factors for all shoots were significantly different from unity, yet almost identical for the two indices.

Our measurements and computations indicate that (spherically averaged) shoot PRI is mostly determined by needle PRI (Fig. 1a): using the average needle spectrum when scaling from needle to shoot level produces unrealistic results ($\mathrm{PRI} \simeq -0.04$) with little between-shoot variation. Needle NDVI values, on the other hand, show much less relative variation (Fig. 1b, Table I) compared with PRI. Scaling to shoot level decreases variation even further. Using the average needle NDVI in the scaling model produces variation similar to that recorded in measurements or obtained from model containing actual needle measurements (Fig. 1b). Thus, for NDVI, the scaling is determined by shoot-level structure, not needle optical properties.

The differences in the scaling properties of PRI and NDVI can be explained by the origins of the variation in $\omega_n(\lambda)$. For the ten shoots, PRI at needle level contained more information than NDVI and this information was transfered to shoot level. The high correlation between ω_n and ω_{sh} at the two PRI wavelengths (Table I) indicates that variation in shoot PRI is, similarly to that of a needle, mostly due to variations in needle pigment concentrations [23], [24] for the ten shoots which had grown in different light conditions. The range in PRI among the needles of the ten measured shoots is relatively large, similar to the seasonal variation in Scots pine needle PRI in Hyytiälä, Finland [24]. We therefore expect that the variation in PRI described here covers most of the natural and geographical variation for this species.

The between-shoot variation in NDVI_{sh} is smaller than that for PRI_{sh} (Table I). This, together with the lack of correlation between NDVI_n and NDVI_{sh}, indicates that the (relatively small) variation in NDVI_n is indeed caused by natural fluctuations and the NDVI_n values for all shoots are not different considering the measurement accuracy. Therefore, the small variation in the modeled NDVI_{sh} evident in Fig. 1b is mostly caused by shoot structure.

The overall accuracy of the scaling model based on p-theory varies. Naturally, the accuracy of the p-theory in scaling the indices using (5) is limited by the overall performance of the theory in predicting shoot scattering. Although the applicability of the theory has been demonstrated experimentally [21], p-theory does not explicitly take into account the intricate details of how photons are scattered within shoots, e.g., the spectral variation in needle scattering directionality. However, for both PRI and NDVI, the model (5) predicts (generally correctly) that the absolute value of shoot-level NDI_{sh} is larger than the corresponding needle-level value, NDI_n. The model underestimates the change for PRI and overestimates it for NDVI. This can be explained by the fact that the recollision probability p is not exactly constant for the entire needle albedo range covered by the two indices. Additionally, the measurement protocol does not guarantee that the initial PRI for needles and shoots is exactly equal as we used sister-shoots for the needle measurements.

The changes in PRI caused by xantophyll cycle pigments happen on the time scale of a few minutes [1] and had most likely already taken place while we adjusted the shoot in the light beam before making any spectral measurements. Longer-term PRI changes may occur due to adjustments in other leaf pigment pools. We analyzed the recorded spectra for each shoot and found no evident temporal trends in its key spectral characteristics during the measurements [14]. Thus, we conclude that the pools of pigments determining the optical properties of needles were sufficiently stable throughout the experiment. However, the detached shoots were exposed to high irradiance for elongated times (about one hour for shoots, more than ten minutes for needles) with an unknown effect on PRI. Therefore, in the light of the many causes of uncertainty discussed above, we consider the results in Fig. 1 satisfactory.

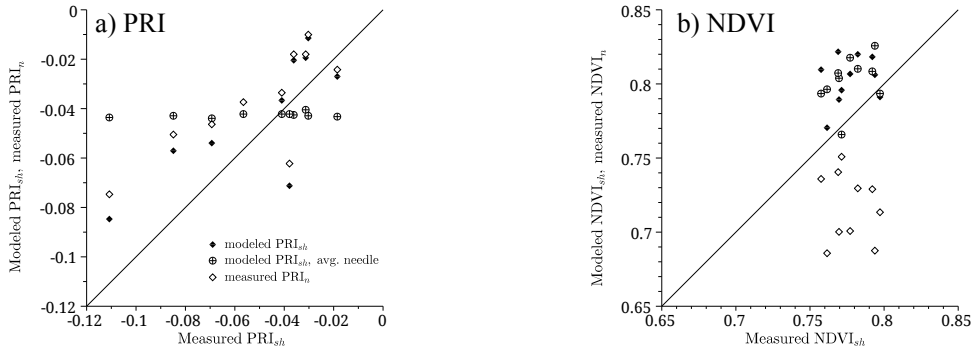

Figure 1. The relationship between spherically averaged needle and shoot-level indices, and results of modeling a) PRI and b) NDVI using (5).

Table I
BETWEEN-SHOOT VARIATION IN NEEDLE (ω_n) AND SHOOT (ω_{sh}) SPECTRAL ALBEDO DESCRIBED USING STANDARD DEVIATION (STD), AND THE PEARSON'S CORRELATION COEFFICIENT R BETWEEN SPECTRAL ALBEDOS AT DIFFERENT WAVELENGTHS, NORMALIZED DIFFERENCE INDICES (NDI), AND NEEDLE SPECTRAL ALBEDO AT 570 NM.

Wavelength λ	STD(ω_n)		STD(ω_{sh})		R between		
(nm)	abs.	rel.	abs.	rel.	$\omega_n(\lambda)$ & $\omega_{sh}(\lambda)$	$\omega_n(\lambda)$ & $\omega_n(570)$	$\omega_{sh}(\lambda)$ & $\omega_{sh}(570)$
531	0.028	0.11	0.028	0.16	0.79	0.95	0.94
570	0.036	0.13	0.030	0.15	0.81	1.00	1.00
680	0.015	0.10	0.010	0.10	0.03	0.72	0.53
780	0.013	0.01	0.068	0.09	0.28	0.26	0.81
NDI	STD(NDI$_n$)		STD(NDI$_{sh}$)		NDI$_n$&NDI$_{sh}$	NDI$_n$&$\omega_n(570)$	NDI$_{sh}$&$\omega_{sh}(570)$
PRI	0.021	–0.56	0.023	–0.56	0.78	–0.54	–0.11
NDVI	0.023	0.03	0.014	0.02	–0.16	–0.71	0.20

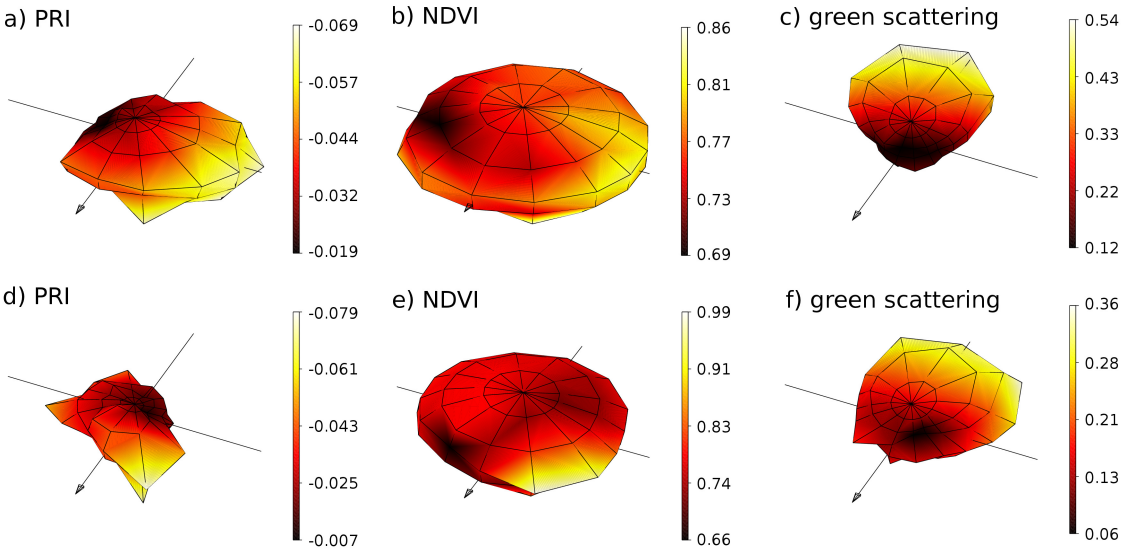

Figure 2. Shoot-level vegetation indices and green (550–565 nm) scattering coefficient as functions of viewing angle. The arrow indicates direction of incident radiation. Shoot axis was approximately parallel to the axis drawn from upper-left to lower-right. Plotted shapes correspond to the directional indices PRI$_{sh}(\Omega)$ (a,d) and NDVI$_{sh}(\Omega)$ (b,e), and the shoot directional scattering coefficient $\omega_{sh}(\Omega)$. Colors convey the same information as the shape. Direction of illumination is indicated by the arrow in each subplot. Results for two shoots (a–c, d–f).

Table II
CORRELATION OF THE DIRECTIONAL VARIATION IN NDI(Ω) WITH SPECTRAL AND DIRECTIONAL PREDICTORS. $N_{\alpha=0.05}$ IS THE NUMBER OF SHOOTS FOR WHICH THE PARTICULAR REGRESSION COEFFICIENT WAS SIGNIFICANT AT $\alpha = 0.05$; N_+ IS THE NUMBER OF SHOOTS FOR WHICH $R > 0$.

predictor variable	PRI Pearson's R (R_{PRI}) min	max	median	$N_{\alpha=0.05}$	N_+	NDVI Pearson's R (R_{NDVI}) min	max	median	$N_{\alpha=0.05}$	N_+
$\omega_{sh}(560,\Omega)$	–0.03	0.51	0.32	9	9	–0.56	–0.25	–0.35	10	0
$\omega_{sh}(680,\Omega)$	0.10	0.58	0.50	9	10	–0.80	–0.47	–0.67	10	0
$\omega_{sh}(780,\Omega)$	–0.07	0.42	0.20	5	9	–0.52	–0.07	–0.17	4	0
$\cos(\vartheta)$, $\vartheta < 90°$	–0.56	–0.04	–0.28	5	0	–0.16	0.32	0.08	1	6
$\cos(\vartheta)$, $\vartheta > 90°$	–0.27	0.31	0.02	1	6	–0.24	0.40	0.19	4	6

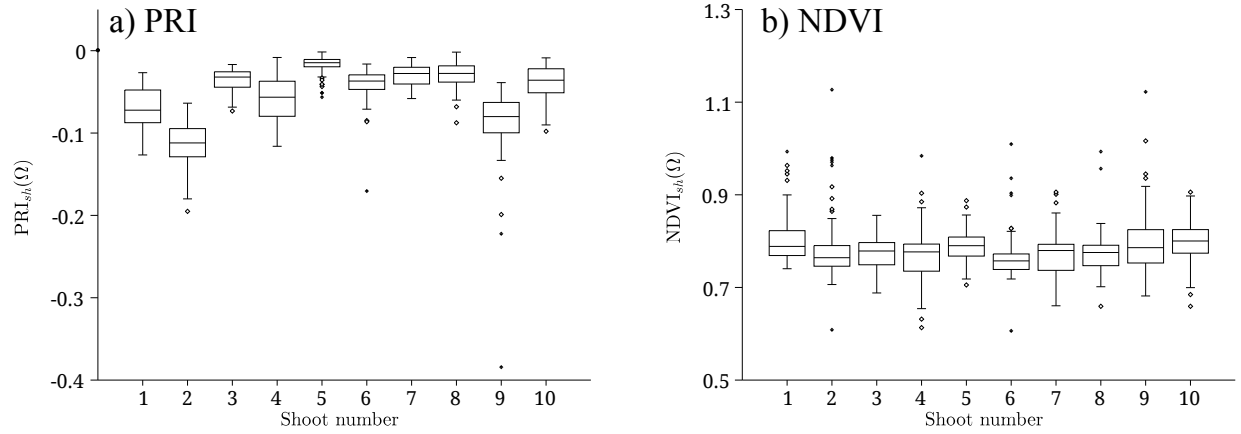

Figure 3. Box plots of a) PRI$_{sh}(\Omega)$ and b) NDVI$_{sh}(\Omega)$ for ten study shoots. The plots present the median NDI$_{sh}(\Omega)$ values as well as 25% and 75% quantiles, minimum and maximum values, and outliers (determined based on their distance from the quantiles).

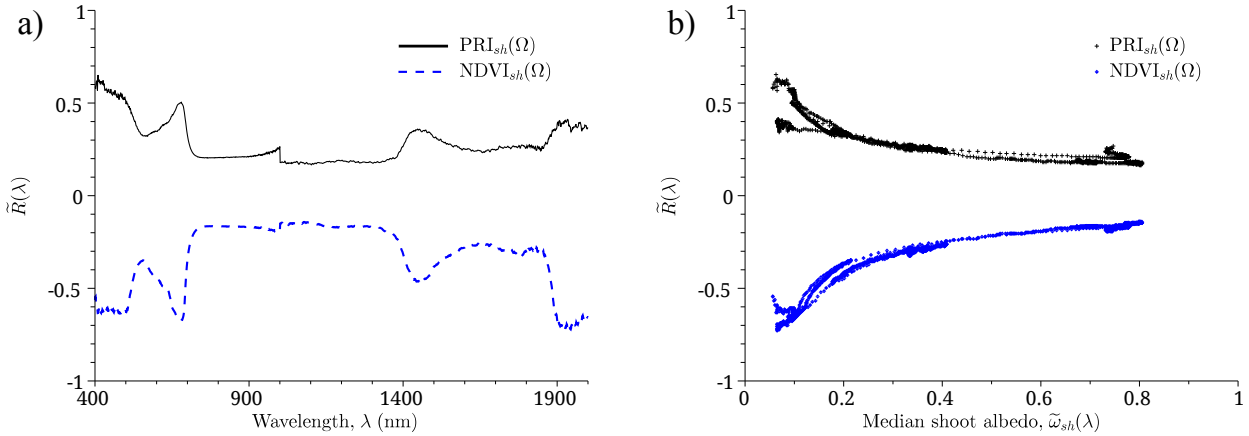

Figure 4. Spectral variation in median Pearson's correlation coefficients ($\widetilde{R}_{\mathrm{PRI}}(\lambda)$ and $\widetilde{R}_{\mathrm{NDVI}}(\lambda)$) between the directional shoot scattering coefficient $\omega_{sh}(\lambda,\Omega)$ and NDIs (PRI$_{sh}(\Omega)$ and NDVI$_{sh}(\Omega)$): a) $\widetilde{R}_{PRI}$ and $\widetilde{R}_{NDVI}$ as functions of wavelength, and b) $\widetilde{R}_{\mathrm{PRI}}$ and $\widetilde{R}_{\mathrm{NDVI}}$ as functions of median shoot scattering coefficient for all wavelengths.

B. Directional dependence of PRI and NDVI

An illustration of the directionality of both vegetation indices, PRI$_{sh}(\Omega)$ and NDVI$_{sh}(\Omega)$, as well as shoot spectral-directional scattering coefficient in green (between 550 and 565 nm) is given in Fig. 2. Two shoots were selected for this illustration, one producing an almost isotropic PRI (Fig. 2a–c) and one with a strong directional peak (Fig. 2d–f). These two shoots represent the typical range in the scattering properties among the ten sampled shoots (Fig. 3). For NDVI (Figure 3b), some of the outliers exceed unity thus indicating negative reflectance values measured in red for some directions caused by measurement noise.

Directional variation in PRI$_{sh}(\Omega)$ is similar in range to between-shoot variation (Fig. 3a), while between-shoot variation in NDVI$_{sh}(\Omega)$ is considerably smaller than variation for individual shoots (Fig. 3b). The directional variations in both indices are correlated with the directional shoot scattering coefficient $\omega_{sh}(\lambda,\Omega)$ in many parts of the analyzed spectrum (Fig. 4). The correlation coefficient of $\omega_{sh}(\lambda,\Omega)$ and PRI$_{sh}(\Omega)$ was always positive, i.e., in the directions where the shoot looked brighter, it also seemed to have a higher (i.e, less negative) PRI. The opposite was true for NDVI: scattering coefficient and NDVI were always correlated negatively. The spectra of both $\left|\widetilde{R}_{\mathrm{PRI}}(\lambda)\right|$ and $\left|\widetilde{R}_{\mathrm{NDVI}}(\lambda)\right|$ strongly resemble that of the whole shoot (Fig. 4a). This is confirmed by Fig. 4b: the correlation is stronger at the wavelengths where the shoot is darker and the median correlation coefficients depend clearly and nonlinearly on median shoot albedo.

The correlation is at its weakest in the near infrared (Fig. 4a). However, even at 780 nm where shoot absorption is at its lowest, the correlation remains statistically significant for four (in case of PRI$_{sh}(\Omega)$) or five shoots (in case of NDVI$_{sh}(\Omega)$) (Table II). In green (560 nm) and red (680 nm) parts of the spectrum, where a shoot absorbs more, the correlations are almost exclusively significant (Table II). Although the correlations are significant for many parts of the spectrum, the coefficients of determination remain low: $R^2_{\mathrm{PRI}} < 0.25$, $R^2_{\mathrm{NDVI}} < 0.5$ (Table II).

The correlations between the two NDIs and the scattering angle, on the other hand, are generally not significant for a majority of shoots (Table II). This is further quantified by N_+ in Table II which shows the number of shoots for which the regression was positive (i.e., $R > 0$). For a dependence to be systematic and generally applicable, N_+ has to be either

very small (close to zero) or approaching sample size (in this study, 10). In three out of four cases presented in Table II, the ten shoots are divided almost equally between positive and negative correlations. For the relationships between shoot directional scattering coefficient and $\mathrm{NDI}_{sh}(\Omega)$ at all three wavelengths presented in Table II, the sign of the correlation coefficient varies rarely between individual shoots.

Based on the same shoot scattering measurements it was previously shown [14] that $\omega_{sh}(\lambda, \Omega)$ depends strongly on the scattering angle, especially in the backward-scattering hemisphere ($\vartheta > 90°$). Indeed, average shoot scattering was fitted well by an isotropic-Lambertion model where, in the backward directions, isotropic scattering was accompanied by a component linear with $\cos\vartheta$. The correlation between $\omega_{sh}(\lambda, \Omega)$ and $\cos\vartheta$ was statistically significant for $\vartheta > 90°$ at the significance level $\alpha = 0.05$ almost universally across the whole spectrum [14]. In the forward scattering directions, this correlation was usually insignificant.

Based on earlier research [14] and our analysis, shoot scattering is correlated with both the cosine of scattering angle ϑ (for $\vartheta > 90°$) and the two NDIs. At the same time, NDIs and $\cos\vartheta$ are generally uncorrelated. This decoupling of $\mathrm{NDI}_{sh}(\Omega)$ and $\cos\vartheta$ allows to analyze the physical mechanisms determining the specific isotropic scattering patterns of conifer shoots: a possible explanation for the decoupling is that the directionality in $\mathrm{NDI}_{sh}(\Omega)$ is caused by a mechanism different than that dominating the directionality of the spectral shoot scattering coefficient, $\omega_{sh}(\lambda, \Omega)$.

We suggest that this mechanism is specular reflection on needle surfaces. Indeed, specular reflection is generally assumed to be small [25] and cannot be responsible for the strong shoot scattering directionality reported by Mõttus et al. [14]. Only at wavelengths where the needle interior absorbs almost all light entering it, is specular reflection expected to provide a significant contribution to needle albedo. Accordingly, our measurements show that the correlation coefficients $\widetilde{R}_{\mathrm{PRI}}(\lambda)$ and $\widetilde{R}_{\mathrm{NDVI}}(\lambda)$ are functions of needle albedo with stronger correlations at wavelengths where the needles absorb more (Figure 4, Table II). The correlation between directional scattering coefficient and directional NDIs does not disappear completely in NIR where shoots absorb very little radiation. This can be explained by the small, yet non-zero, contribution of specular reflection at these wavelengths. Also, the signs of R_{PRI} and R_{NDVI} agree with this interpretation. If the signal at wavelengths where the needles absorb was largely contributed by specular reflection, the value of any NDI_{sh} in this direction would be closer to zero than in other directions. Thus, if the directionality of indices was caused by specular scattering, $R_{\mathrm{PRI}} > 0$ and $R_{\mathrm{NDVI}} < 0$, which is in agreement with our results.

Based on Fig. 3, the directional variation in PRI is too strong to be simply ignored in analyzing multiangular measurements. However, the directionality of scattering as a function of view and illumination angles is difficult to quantify. If the directionality of PRI of individual shoots is indeed driven mainly by specular reflection, it carries no information on needle biochemistry and depends on simple geometric considerations: view and illumination angles, and the angular distribution of needle surfaces. However, to correct for specular effects, a quantitative model relating shoot specular scattering to view direction has to be developed. For a correct interpretation of directional PRI signal, the quantitative model has to include canopy structural effects also on scales other than the shoot.

IV. Conclusions

PRI scales reasonably well between two different structural levels (needles and shoots) in coniferous canopies. Scaling tends to increase the absolute value of the index with structural level while retaining the biochemical information potentially contained in the index. Mathematically, the conversion factor for scaling a normalized difference index (such as PRI) between canopy structural levels is a simple function of two quantities: (i) the harmonic mean of the spectral albedo of the smaller structural level at the wavelengths used in the index, and (ii) the spectrally invariant photon recollision parameter p. The directional dependence of PRI is of the order of between-shoot variation and has to be considered when analyzing multiangular spectral measurements. The variations in the index with view angle may be largely caused by specular reflectance on needle surfaces.

V. Acknowledgements

We are grateful to the staff at RSL and Prof. Michael Schaepman for making the measurements possible, and to Dr. Lea Hallik (Estonian University of Life Sciences) for valuable discussions on PRI.

References

[1] J. A. Gamon, J. Peñuelas, and C. B. Field, "A narrow-waveband spectral index that tracks diurnal changes in photosynthetic efficiency," *Remote Sensing of Environment*, vol. 41, no. 1, pp. 35–44, 1992.

[2] T. Hilker, F. G. Hall, N. C. Coops, A. Lyapustin, Y. Wang, Z. Nesic, N. Grant, T. A. Black, M. A. Wulder, N. Kljun, C. Hopkinson, and L. Chasmer, "Remote sensing of photosynthetic light-use efficiency across two forested biomes: Spatial scaling," *Remote Sensing of Environment*, vol. 114, no. 12, pp. 2863–2874, 2010.

[3] M. F. Garbulsky, J. Peñuelas, J. Gamon, Y. Inoue, and I. Filella, "The photochemical reflectance index (PRI) and the remote sensing of leaf, canopy and ecosystem radiation use efficiencies. A review and meta-analysis," *Remote Sensing of Environment*, vol. 115, no. 2, pp. 281–297, 2011.

[4] J. Grace, C. Nichol, M. Disney, P. Lewis, T. Quaife, and P. Bowyer, "Can we measure terrestrial photosynthesis from space directly, using spectral reflectance and fluorescence?" *Global Change Biology*, vol. 13, no. 7, pp. 1484–1497, 2007.

[5] R. Hernández-Clemente, R. M. Navarro-Cerrillo, L. Suárez, F. Morales, and P. J. Zarco-Tejada, "Assessing structural effects on PRI for stress detection in conifer forests," *Remote Sensing of Environment*, vol. 115, no. 9, pp. 2360–2375, 2011.

[6] M. Schlerf and C. Atzberger, "Vegetation structure retrieval in beech and spruce forests using spectrodirectional satellite data," *IEEE Journal of Selected Topics in Applied Earth Observations and Remote Sensing*, vol. 5, no. 1, pp. 8–17, 2012.

[7] K. Niemann, G. Quinn, D. Goodenough, F. Visintini, and R. Loos, "Addressing the effects of canopy structure on the remote sensing of foliar chemistry of a 3-dimensional, radiometrically porous surface," *IEEE Journal of Selected Topics in Applied Earth Observations and Remote Sensing*, vol. 5, no. 2, pp. 584–593, 2012.

[8] Y. Knyazikhin, M. Schull, P. Stenberg, M. Mõttus, M. Rautiainen, Y. Yang, A. Marshak, P. Carmona, R. Kaufmann, P. Lewis, M. Disney, V. Vanderbilt, A. Davis, F. Baret, S. Jacquemoud, A. Lyapustin, and R. Myneni, "Hyperspectral remote sensing of foliar nitrogen content," *Proceedings of the National Academy of Sciences of the United States of America*, vol. 110, no. 3, pp. 811–812, 2013.

[9] P. Oker-Blom and S. Kellomäki, "Effect of grouping of foliage on the within-stand and within-crown light regime: Comparison of random and grouping canopy models," *Agricultural Meteorology*, vol. 28, no. 2, pp. 143–155, 1983.
[10] T. Nilson and J. Ross, *The use of remote sensing in the modeling of forest productivity*. Kluwer Academic Publishers, Dordrecht, 1997, ch. Modeling radiative transfer through forest canopies: implications for canopy photosynthesis and remote sensing, pp. 23–60.
[11] A. Cescatti, "Modelling the radiative transfer in discontinuous canopies of asymmetric crowns. I. Model structure and algorithms," *Ecological Modelling*, vol. 101, no. 2–3, pp. 263–274, 1997.
[12] T. Hilker, A. Lyapustin, F. G. Hall, Y. Wang, N. C. Coops, G. Drolet, and T. A. Black, "An assessment of photosynthetic light use efficiency from space: Modeling the atmospheric and directional impacts on PRI reflectance," *Remote Sensing of Environment*, vol. 113, no. 11, pp. 2463–2475, 2009.
[13] E. Middleton, Y.-B. Cheng, T. Hilker, T. Black, P. Krishnan, N. Coops, and K. Huemmrich, "Linking foliage spectral responses to canopy-level ecosystem photosynthetic light-use efficiency at a Douglas-fir forest in Canada," *Canadian Journal of Remote Sensing*, vol. 35, no. 2, pp. 166–188, 2009.
[14] M. Mõttus, M. Rautiainen, and M. E. Schaepman, "Shoot scattering phase function for Scots pine and its effect on canopy reflectance," *Agricultural and Forest Meteorology*, vol. 154-155, no. 1, pp. 67–74, 2012.
[15] C. J. Tucker, "Red and photographic infrared linear combinations for monitoring vegetation," *Remote Sensing of Environment*, vol. 8, pp. 127–150, 1979.
[16] G. le Maire, C. François, K. Soudani, D. Berveiller, J.-Y. Pontailler, N. Bréda, H. Genet, H. Davi, and E. Dufrêne, "Calibration and validation of hyperspectral indices for the estimation of broadleaved forest leaf chlorophyll content, leaf mass per area, leaf area index and leaf canopy biomass," *Remote Sensing of Environment*, vol. 112, no. 10, pp. 3846–3864, 2008.
[17] B.-C. Gao, "NDWI - a normalized difference water index for remote sensing of vegetation liquid water from space," *Remote Sensing of Environment*, vol. 58, no. 3, pp. 257–266, 1996.
[18] R. Fensholt and I. Sandholt, "Derivation of a shortwave infrared water stress index from MODIS near- and shortwave infrared data in a semiarid environment," *Remote Sensing of Environment*, vol. 87, no. 1, pp. 111–121, 2003.
[19] A. Gitelson, Y. Kaufman, R. Stark, and D. Rundquist, "Novel algorithms for remote estimation of vegetation fraction," *Remote Sensing of Environment*, vol. 80, no. 1, pp. 76–87, 2002.
[20] S. Dangel, M. Verstraete, J. Schopfer, M. Kneubühler, M. Schaepman, and K. Itten, "Toward a direct comparison of field and laboratory goniometer measurements," *IEEE Transactions on Geoscience and Remote Sensing*, vol. 43, no. 11, pp. 2666–2675, 2005.
[21] M. Rautiainen, M. Mõttus, L. Yáñez Rausell, L. Homolová, Z. Malenovský, and M. Schaepman, "A note on upscaling from coniferous needle spectral albedo to shoot spectral albedo," *Remote Sensing of Environment*, vol. 117, pp. 469–474, 2012.
[22] S. Smolander and P. Stenberg, "A method to account for shoot scale clumping in coniferous canopy reflectance models," *Remote Sensing of Environment*, vol. 88, no. 4, pp. 363–373, 2003.
[23] T. Hilker, N. Coops, F. Hall, T. Black, M. Wulder, Z. Nesic, and P. Krishnan, "Separating physiologically and directionally induced changes in PRI using BRDF models," *Remote Sensing of Environment*, vol. 112, no. 6, pp. 2777–2788, 2008.
[24] A. Porcar-Castell, J. Garcia-Plazaola, C. Nichol, P. Kolari, B. Olascoaga, N. Kuusinen, B. Fernández-Marín, M. Pulkkinen, E. Juurola, and E. Nikinmaa, "Physiology of the seasonal relationship between the photochemical reflectance index and photosynthetic light use efficiency," *Oecologia*, vol. 170, pp. 313–323, 2012.
[25] L. Grant, "Diffuse and specular characteristics of leaf reflectance," *Remote Sensing of Environment*, vol. 22, no. 2, pp. 309–322, 1987.

Matti Mõttus received the M.Sc. degree in physics in 2000, and the PhD degree in environmental physics in 2004 from the University of Tartu, Estonia. Since then, he has worked in Tartu Observatory, Estonia, and University of Helsinki, Finland. He is presently a researcher at the Department of Geosciences and Geography of the University of Helsinki. His current research focuses on imaging spectroscopy and radiative transfer in vegetation canopies.

Miina Rautiainen received the M.Sc. degree in biology from the University of Turku, Finland in 2002 and the PhD degree (with distinction) in forest science from the University of Helsinki, Finland in 2005. She is currently an Academy of Finland Research Fellow in the Department of Forest Sciences, University of Helsinki, Finland. Her current research interests include the development and application of forest reflectance models and remote sensing of forest structure.